Spin-state modulation of molecular Fe III complexes via inclusion in halogen-bonded supramolecular networks

Ie-Rang Jeon, Olivier Jeannin, Rodolphe Clérac, Mathieu Rouzières, Marc Fourmigué

Spin-State Modulation of Molecular Fe^{III} Complexes via Inclusion in Halogen-Bonded Supramolecular Networks†

Ie-Rang Jeon,*[,a] Olivier Jeannin,[a] Rodolphe Clérac,[b,c] Mathieu Rouzières,[b,c] and Marc Fourmigué*[,a]

The cationic complex $[Fe(qsal)_2]^+$ (Hqsal = N-(8-quinolyl)salicylaldimine) is encapsulated in anionic halogen-bonded 1D and 2D networks derived from *sym*-triiodotrifluorobenzene, $[(C_6F_3I_3)Cl]^-$ and $[(C_6F_3I_3)I]^-$. Structural analysis and magnetic measurements show that the spin-state of this complex can be modulated by inclusion in supramolecular host frameworks.

Physical properties of molecules can potentially undergo drastic modulation through their rational assembly with other molecular building blocks in the solid state. Such a crystal engineering approach in materials chemistry is of paramount importance toward the programmation and the optimization of the desired properties.[1] While using hydrogen bonding is by far the most adopted strategy to control the auto-organization of molecular entities,[2] halogen bonding interactions have recently proven their efficiency in guiding supramolecular organization.[3] In particular, the nature and the strength of this interaction has been demonstrated to be highly directional and modulable, which allow them to outperform hydrogen bonding in certain recognition processes.[4] Despite the successful demonstration of its structural role, the active participation of halogen bonding to control electronic properties has been essentially limited to molecular conductors and has yet to be explored in magnetic systems.[5]

In selecting functional paramagnetic molecules, spin crossover systems that undergo an electronic equilibrium between two spin states represent ideal platforms to investigate, in conjunction with halogen bonding-based crystal engineering. Indeed, spin crossover is often accompanied by drastic changes in structural, optical, magnetic and electrical responses, providing potential uses in applications such as molecule-based switches and memories.[6] Specifically, the manifestation of spin crossover in the solid state is intimately related to the modes of interactions between the molecular entities undergoing the spin-state change. As such, understanding the relationship between different types of intermolecular interactions and spin crossover behavior still represents a formidable challenge toward predicting and regulating the nature of the spin equilibrium. Numerous synthetic parameters that can result in modification of the intermolecular interactions, have been investigated to date, including functional groups of ligands, counter ions, and solvent molecules.[7]

Despite these significant advances of crystal engineering in spin crossover systems, the effect of halogen bonding has barely been explored.[8] Those observed to date are limited to interactions between sites on two ligands or between a ligand and a discrete molecule. In some of them, the involved halogen bonding is likely very weak. Furthermore, no example integrates spin crossover complexes into halogen-bonded supramolecular frameworks yet.

Herein, we report the incorporation of molecular Fe^{III} cations in anionic halogen-bonded supramolecular networks, as a means to organize functional molecular entities and modulate their electronic properties. To our knowledge, this three-component co-crystal system represents the first example of using a halogen-bonded network to modulate the spin of a guest molecule.

We selected the cationic $[Fe(qsal)_2]^+$ spin crossover moiety as a

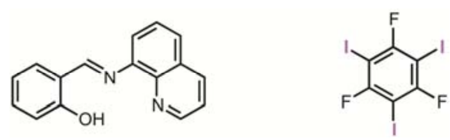

Figure 1. N-(8-quinolyl)salicylaldimine (Hqsal, left) and *sym*-triiodotrifluorobenzene (right) highlighting threefold halogen bond donating ability of the molecule.

[a] Institut des Sciences Chimiques de Rennes, Université de Rennes 1 & CNRS UMR 6226, Campus Beaulieu, 35042 Rennes, France.
E-mail: ie-rang.jeon@univ-rennes1.fr & marc.fourmigue@univ-rennes1.fr
[b] CNRS, CRPP, UPR 8641, 33600 Pessac, France.
[c] Univ. Bordeaux, CRPP, UPR 8641, 33600 Pessac, France.

†Electronic Supplementary Information (ESI) available: Experimental details, crystallographic data, crystal structures, additional magnetic data, and crystallographic information files (CIF). CCDC 1537574–1537578. See DOI: 10.1039/x0xx00000x

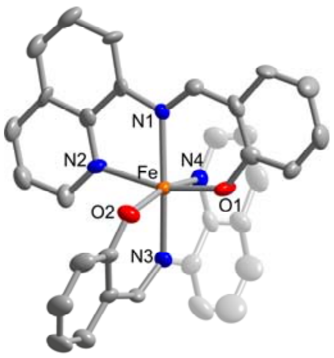

Figure 2. X-ray crystal structure of $[Fe(qsal)_2]^+$ in **1**, collected at T = 298 K. Brown, red, blue, and gray ellipsoids, shown at the 50% probability level, represent Fe, O, N, and C atoms, respectively; H atoms are omitted for clarity.

functional molecular guest that can be controlled by a halogen-bonded network. The solid-state magnetic properties of the chloride and iodide salts have been previously reported to reveal a high-spin and a low-spin state, respectively, in a temperature range between 2 and 300 K.[9,10] In these salts, the counter anion dependence of the spin-state implies that the two magnetic states are likely placed close in energy.[11] Indeed, several analogous salts with other anions have been reported to exhibit spin crossover properties.[7,12] To target a halogen-bonded self-assembly, we specifically focused on the $[Fe(qsal)_2]X$ (X = Cl and I) salts owing to the great efficiency of halide anions to act as a halogen bond acceptor. Particularly, the difference in ionic radius and electron density between Cl^- and I^- enables us to vary the strength and the length of envisioned halogen bonds. In parallel, *sym*-trifluorotriiodobenzene ($C_6F_3I_3$) was chosen to serve as a halogen bond donor to deliberately build a network (Figure 1), since we and others have proven the efficient construction of supramolecular structures using this three-fold iodoperfluorocarbon molecule in the presence of naked halide anions.[13]

The synthesis of the molecular Fe^{III} salts proceeded following modified literature procedures.[9] Reaction of $FeCl_3$ with *in-situ* formed Hqsal in MeOH, followed by treatment of a stoichiometric amount of NEt_3, afforded a dark brown solution. Subsequent slow evaporation of the MeOH solution yielded dark brown microcrystalline solid. Recrystallization of this solid from MeOH yielded needle-shaped crystals of $[Fe(qsal)_2]Cl{\cdot}MeOH{\cdot}H_2O$ (**1**), suitable for single-crystal X-ray diffraction. On the other hand, the treatment of a mixture of KI and NEt_3 into the MeOH solution of $FeCl_3$ and Hqsal afforded dark brown needle-shaped crystals of $[Fe(qsal)_2]I{\cdot}H_2O$ (**2**) instantaneously.[10]

To obtain halogen-bonded co-crystals, subsequent reaction of **1** with 1.4 eq. of $C_6F_3I_3$ in MeCN yielded dark needle-shaped crystals of $[Fe(qsal)_2][(C_6F_3I_3)Cl]$ (**3**). Similarly, treatment of the MeCN solution of **1** by a mixture of 17 eq. of $C_6F_3I_3$ and 1.0 eq. of KI in MeCN gave dark elongated hexagonal-shaped crystals of $[Fe(qsal)_2][(C_6F_3I_3)I]{\cdot}MeCN$ (**4**). Owing to the low solubility of **2** in most organic solvents, the synthesis of **4** was performed by slowly diffusing solutions of $[Fe(qsal)_2]Cl$, KI, and $C_6F_3I_3$, which involves possibilities to form other crystalline materials as a byproduct. We have indeed noted that a slight modification in stoichiometry resulted in a mixture of **2** and **4**. As such, the bulk purity of the samples for further physical analyses were systematically verified by elemental microanalysis and powder X-ray diffraction (Figure S1).

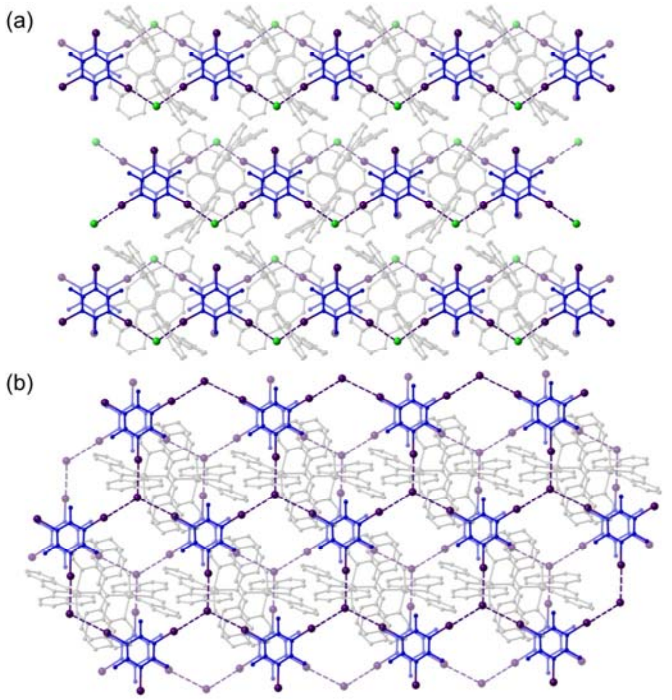

Figure 3. X-ray crystal structure of $[Fe(qsal)_2][(C_6F_3I_3)Cl]$ in **3** (a) and $[Fe(qsal)_2][(C_6F_3I_3)I]$ in **4** (b), as viewed along the crystallographic *a* and *c* axes, respectively. The $[Fe(qsal)_2]^+$ cationic complexes and the $[(C_6F_3I_3)X]^-$ anionic halogen-bonded networks are shown in gray and blue, respectively, for clarity. Halogen bonding interactions are highlighted as the purple dashed lines with I and Cl atoms in purple and green spheres.

The structure of $[Fe^{III}(qsal)_2]^+$ in compound **1** reveals an Fe^{III} center residing in a distorted octahedral coordination environment, surrounded by four nitrogen and two oxygen donor atoms from two qsal ligands (Figure 2). At 298 K, the average Fe–N and Fe–O distances are 2.143(9) and 1.902(7) Å, respectively. The observed bond metrics significantly differ from those of 1.963(4) and 1.872(3) Å for **2**, that was previously reported as a low-spin Fe^{III},[10] unambigously indicating a high-spin Fe^{III} configuration for **1**. Note that, to our knowledge, **1** is the first example involving the molecular $[Fe^{III}(qsal)_2]Cl$ salt that is structurally characterized. The $[Fe^{III}(qsal)_2]^+$ cations in **1** and **2** feature short contacts with adjacent complexes by π···π interactions, revealing phenyl embrace motifs (Figure S2).

The structure of **3** consists of molecular $[Fe^{III}(qsal)_2]^+$ cations arranged in an 1D zigzag anionic network $[(C_6F_3I_3)Cl]^-$ that propagates along the crystallographic *b* axis (Figure 3a). Here, both $C_6F_3I_3$ and Cl^- behave as a ditopic halogen bond donor and acceptor with the I···Cl^-···I angle of 109.38(7)°. The I···Cl^- distances of 3.086(2) and 3.115(2) Å, that are 18 and 17% shorter than the sum of van der Waals and Pauling ionic radii, respectively, indicates the strength of this halogen bonding interaction. An individual chain is paired with the adjacent one through offset face-to-face π stacking between $C_6F_3I_3$ molecules, that features ca. 60° of rotation to one another to avoid steric hindrance between iodine atoms (Figure S3). Between the pair of chains, the $[Fe^{III}(qsal)_2]^+$ complexes are arranged as a dimerized unit through π stacking between quinoline and phenyl rings of the equivalent ligands (Figure S4). These dimerized units, separated by the halogen-bonded network,

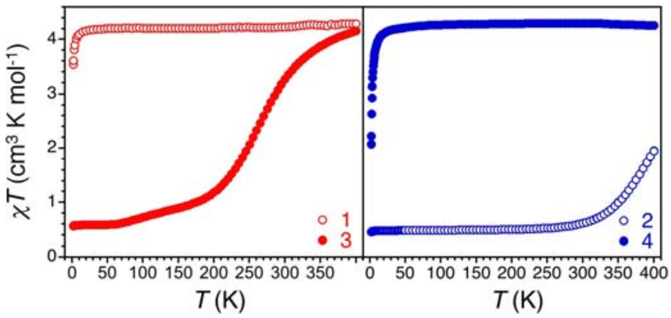

Figure 4. Variable-temperature dc magnetic susceptibility (χ = M/H per mole of compound) data for **1**–**4** shown as a plot of χT vs T, collected under an applied field of 1 T from 400 to 100 K and 0.1 T below 100 K at a temperature sweeping rate of 0.7 K/min.

exhibits no significant further nonconvalent interactions with adjacent Fe complexes. The average Fe–N and Fe–O distances at 298 K are 2.077(7) and 1.891(7) Å, which likely represents in **3** a partial portion of Fe^{III} centres in a high-spin state. Accordingly, those at 100 K are 1.873(5) and 1.967(6) Å, unambigously indicating a low-spin Fe^{III} configuration and implying that **3** undergoes spin crossover.

The replacement of Cl^- by I^- in **4** resulted in a fully different halogen bonding organisation, revealing a 2D honeycomb-like network, where both $C_6F_3I_3$ and I^- anion are now tritopic (Figure 3b). The I···I^- distances are 3.494(2), 3.554(2), and 4.042(2) Å, revealing 16, 15, and 3% reduction from the sum of the van der Waals and ionic radii. The central I^- anion is ca. 1 Å off from the plane formed by three iodine, making the layer severely undulated (Figure S5). Similar to that of **3**, the layer is paired with the adjacent one through π stacking, resulting in a staggered arrangement of the layers that stack along the crystallographic *c* axis. The $[Fe^{III}(qsal)_2]^+$ complexes are dimerized similar to that of **3** between the paired layers. For **4**, the dimer unit is engaged in an additional π interaction between phenyl rings, affording an extensively interacting network (Figure S5). The average Fe–N and Fe–O distances at 298 K are 2.139(5) and 1.910(6) Å, which can be assigned to a high-spin Fe^{III} ion configuration.

In the structures of **3** and **4**, both Cl^- and I^- anions actively participate in halogen bonding with $C_6F_3I_3$ donor molecules to construct the anionic supramolecular networks. Particularly, the formation of the halogen-bonded network modified the self-assembly of $[Fe^{III}(qsal)_2]^+$ complexes relative to that of **1** and **2**, resulting in geometrically identical dimerized $[Fe]_2$ units for **3** and **4**. The Cl^- and $C_6F_3I_3$ in **3** behaved as ditopic units leading to a 1D network, while both are tritopic moieties in **4** yielding a 2D layer. The smaller size of Cl^- is likely the reason of the incapability to form a 2D framework while accomodating the large dimerized $[Fe]_2$ units. To illustrate this, the Fe···Fe distance of $[Fe]_2$ in **4** is greatly reduced compared to those in **1**–**3** (Table S2), and one of the I···I^- interactions is significantly weaker than the two others. As such, we reasoned that the hypothetical third I···Cl^- interaction in **3** was potentially overcome by the other intermolecular interactions. Indeed, the third iodine atom of $C_6F_3I_3$ features short contacts with the adjacent quinoline rings (Figure S2). As a result, this preferential I···qsal interactions shifted the paired-chain columns along the *a* axis, hindering the formation of the honeycomb-like 2D layers.

To probe the spin-state of $[Fe^{III}(qsal)_2]^+$ complexes in **1**–**4**, variable-temperature magnetic susceptibility data were collected on solid samples, and the resulting plot of χT vs T is shown in Figure 4. At 400 K, χT = 4.29 cm^3K/mol for **1** corresponds to the value for a high-spin S = $^5/_2$ Fe^{III} centre with g = 1.98. As temperature is decreased, the data exhibit relatively constant plateau down to 40 K, indicating Fe centres in **1** remain as a high-spin. On the contrary, the compound **3**, consisting of **1** implemented in a halogen-bonded network, exhibits a gradual decrease of the χT product from 4.15 to 0.57 cm^3K/mol, as temperature is decreased from 400 to 2 K. The *S*-shaped curve unambiguously indicates the occurrence of spin crossover in **3**, and a fit based on the ideal solution model estimated the crossover temperature ($T_{1/2}$) at 268(1) K (Figure S6).[14] Note that the anomaly in temperature range between 70 and 200 K was not included in the fit and is likely attributable to the presence of a small amount of a different phase. Despite our efforts effort to identify the potential processes involved, the quality of crystal prohibited the detection of any other phase by conventional X-ray diffraction. Nevertheless, a fit based on an S = $^1/_2$ Brillouin function agreed well with the plot of M vs H at 1.8 K, further confirming a low-spin configuration of **3** (Figure S7).

On the other hand, magnetic data for **2** showed χT = 0.48 cm^3K/mol at T = 20 K, corresponding to a low-spin S = $^1/_2$ Fe^{III} centre with g = 2.26. As temperature is increased, the χT product remains almost constant then show a gradual increase above 250 K to reach a value of 1.96 cm^3K/mol at 400 K, indicating the onset of spin crossover, which has not been fully detected in the previous magnetic measurements.[10] Remarkably, the compound **4**, that accomodates **2** in a 2D halogen-bonded network, remains high-spin in all temperature range, as evidenced by a constant χT value of 4.28 cm^3K/mol down to 40 K. To our knowledge, the halogen-bonded supramolecular network has proven here, for the first time, its ability to act as an efficient crystal engineering tool that can modulate the electronic properties of a metal complex.

To further explore the trend associated with this spin-state modulation, several structural characteristics have been compared across the series **1**–**4**. We have listed local structural parameters that can potentially affect the electronic structure of a metal complex in Table S2. Several relevant parameters were not able to make any reliable correlation with the observed magnetic behavior of the compounds, which is also visualized and compared with other literature examples containing $[Fe(qsal)_2]^+$ units in Figure S8. Nevertheless, it seems that the *trans* N1-Fe-N3 angle (ϕ) needs to be close to 180° to access a low-spin configuration. Indeed, the structure of **3** at 100 K reveals the N1-Fe-N3 angle of 178.4(3)°, that is slightly greater than that of 298 K. The more linear N1-Fe-N3 backbone at 100 K is likely achieved by changing the configuration of the phenyl ring on the qsal ligand, as evidenced by the Fe-O1-C1-C2 torsion angle of 11.3 and 21.1° for T = 100 and 298 K, respectively (Figure S4). In contrast, the structure of **4** features multiple halogen bonding and π interactions that hinder the flexibility of the acrylic backbone, as evidenced by subtle changes in the Fe-O-C-C torsion angles between T = 100 and 298 K, respectively (Table S2). Consequently, this results in the quasi identical N1-Fe-N3 angles of 168.5(1) and 168.1(2)° for T = 100 and 298 K, respectively, which likely trap the high-spin states in **4** (Figure S5). This observation clearly indicates that the spin crossover behavior of these compounds is not soley governed by local structural parameters, and rather directed by the incorporated halogen-bonded networks that dominates the crystal packing. Note that such a crystal packing effect to trap a certain spin-state, albeit in non halogen-bonded systems, have been proposed earlier.[15]

To investigate possible magnetic interactions between molecular Fe^{III} units in compounds **1**–**4**, the low temperature data in the χT vs T plot are further analyzed. The data of **1**–**4** below 60 K exhibit a quasi plateau at χT = 4.29, 0.48, 0.57, and 4.28 cm^3K/mol, respectively, then a decrease at lower temperatures. This thermal behavior indicates the presence of antiferromagnetic intermolecular interactions. Fits of the experimental data using the mean-field approximation estimated the exchange constant zJ' = –0.04 (–0.06), –0.13 (–0.19), –0.07 (–0.10), and –0.15 (–0.22) cm^{-1} (K), respectively, for compounds **1**, **2**, **3**, and **4** (Figure S9).[16] Albeit similar, the obtained results show the most significant intermolecular magnetic coupling in compound **4**, likely related to the extensive intermolecular contacts observed in the structure packing. The presence of significant antiferromagnetic interactions in **4** is further evidenced by an *S*-shaped curve in the *M* vs *H* plot at 1.8 K (Figure S10). The deduced value of the average interactions between $S = {}^5/_2$ spins in **4** is estimated at zJ' = –0.14 cm^{-1} (–0.21 K), which agrees well with the one obtained from the fit to the variable-temperature magnetic susceptibility data.[17]

The foregoing results demonstrate the ability of halogen bonding interactions to modulate the electronic properties of metal complexes. Specifically, the spin crossover behavior of the "naked" molecular $[Fe^{III}(qsal)_2]$X salts can be turned on and off for X = Cl and I, respectively, upon their implementation into 1D and 2D halogen-bonded supramolecular networks. Work is underway to vary halogen bond donors and acceptors in terms of geometry and strength.

This research was supported by the French National Research Agency Grant ANR 16-ACHN-0007. I.R.J., O.J., and M.F. thank the CDIFX and the physical measurement platform in Rennes for the use of X-ray diffractometer and SQUID magnetometer. R.C. and M.R. thank the University of Bordeaux, the CNRS, and the Nouvelle Aquitaine Region.

Notes and references

1 G. R. Desiraju, *Angew. Chem. Int. Ed.*, 1995, **34**, 2311.
2 G. R. Desiraju, *J. Am. Chem. Soc.*, 2013, **135**, 9952.
3 P. Metrangolo, H. Neukirch, T. Pilati and G. Resnati, *Acc. Chem. Res.*, 2005, **38**, 386; F. Mayer and P. Dubois, *CrystEngComm*, 2013, **15**, 3058.
4 G. Cavallo, P. Metrangolo, R. Milani, T. Pilati, A. Priimagi, G. Resnati and G. Terraneo, *Chem. Rev.*, 2016, **116**, 2478, and references therin.
5 M. Fourmigué and P. Batail, *Chem. Rev.*, 2004, **104**, 5379. M. Fourmigué, *Struct. Bond.*, 2008, **126**, 181.
6 P. Gütlich and H. A. Goodwin, *Top. Curr. Chem.*, 2004, **233**, 1; A. Bousseksou, G. Molnar, L. Salmon and W. Nicolazzi, *Chem. Soc. Rev.*, 2011, **40**, 3313; M. A. Halcrow, *Spin-Crossover Materials: Properties and Applications*, John Wiley & Sons, 2013.
7 W. Zhang, F. Zhao, M. Yuan, Z.-M. Wang and S. Gao, *Inorg. Chem.*, 2007, **46**, 2541; B. Li, R.-J. Wei, J. Tao, R.-B. Huang, L.-S. Zheng and Z. Zheng, *J. Am. Chem. Soc.*, 2010, **132**, 1558; J. A. Kitchen, N. G. White, G. N. L. Jameson, J. L. Tallon and S. Brooker, *Inorg. Chem.*, 2011, **50**, 4586; C. Bartual-Murgui, C. Codina, O. Roubeau and G. Aromí, *Chem. Eur. J.*, 2016, **22**, 12767.
8 K. Fukuroi, K. Takahashi, T. Mochida, T. Sakurai, H. Ohta, T. Yamamoto, Y. Einaga and H. Mori, *Angew. Chem. Int. Ed.*, 2014, **53**, 1983; N. Nassirinia, S. Amani, S. J. Teat, O. Roubeau and P. Gamez, *Chem. Commun.*, 2014, **50**, 1003; W. Phonsri, D. J. Harding, P. Harding, K. S. Murray, B. Mourabaki, I. A. Gass, J. D. Cashion, G. N. L. Jameson and H. Adams, *Dalton Trans.*, 2014, **43**, 17509.
9 R. C. Dickinson, W. A. Baker and R. C. Collins, *J. Inorg. Nucl. Chem.*, 1977, **39**, 1531.
10 B. Djukic, H. A. Jenkins, T. Seda and M. T. Lemaire, *Trans. Met. Chem.*, 2013, **38**, 207.
11 B. Djukic, P. A. Dude, F. Razavi, T. Seda, H. A. Jenkins, J. F. Britten and M. T. Lemaire, *Inorg. Chem.*, 2009, **48**, 699.
12 S. Hayami, Z. Z. Gu, H. Yoshiki and A. Fujishima, O. Sato, *J. Am. Chem. Soc.*, 2001, **123**, 11644.
13 S. Triguero, R. Llusar, V. Polo and M. Fourmigué, *Cryst. Growth Des.*, 2008, **8**, 2241; P. Metrangolo, F. Mayer, T. Pilati, G. Resnati and G. Terraneo, *Chem. Commun.*, 2008, 1635; M. C. Pfrunder, A. S. Micallef, L. Rintoul, D. P. Arnold and J. McMurtie, *Cryst. Growth Des.*, 2016, **16**, 681.
14 See P. Atkins, J. De Paula, *Physical Chemistry*, 8th Edition 2006, Oxford University Press, Chapter 5; D. Siretanu, D. Li, L. Buisson, D. M. Bassani, S. M. Holmes, C. Mathonière and R. Clérac, *Chem. Eur. J.*, 2011, **17**, 11704.
15 M. A. Halcrow, *Chem. Soc. Rev.*, 2011, **40**, 4119.
16 B. E. Myers, L. Berger and S. Friedberg, *J. Appl. Phys.*, 1969, **40**, 1149; C. J. O'Connor, *Prog. Inorg. Chem.*, 1982, **29**, 203.
17 L. J. Jongh and A. R. Miedena, *Adv. Phys.*, 1974, **23**, 1.